

Development and Characterization of Vacuum Plasma Sprayed Thin Film Solid Oxide Fuel Cells

M. Lang, R. Henne, S. Schaper, and G. Schiller

(Submitted 3 July 2000)

The vacuum plasma spraying (VPS) process allows the production of thin solid oxide fuel cells (SOFCs) with low internal resistances. This enables the reduction of the cell operating temperature without a significant decrease in power density. Consequently, the long-term stability of the cells can be improved and low-cost materials can be used.

Different material combinations and spray parameter variations were applied to develop thin-film SOFCs, which were plasma sprayed in a consecutive deposition process onto different porous metallic substrates. The use of Laval nozzles, which were developed at the German Aerospace Center (DLR), and the use of conical F4V standard nozzles enable the fabrication of thin gas tight yttria- and scandia-stabilized ZrO₂ (YSZ and ScSZ) electrolyte layers and of porous electrode layers with high material deposition rates. The optimization of the VPS parameters has been supported by laser doppler anemometry (LDA) investigations.

The development of the plasma-sprayed cells with a total thickness of approximately 100 μm requires an overall electrical and electrochemical characterization process of the single layers and of the completely plasma-sprayed cell assembly. The plasma-sprayed cell layers reveal high electrical conductivities. The plasma-sprayed cells show very good electrochemical performance and low internal resistances. Power densities of 300 to 400 mW/cm² at low operating temperatures of 750 to 800 °C were achieved. These cells can be assembled to high performance SOFC stacks with active cell areas up to 400 cm², which can be operated at reduced temperatures and good long-term stability.

Keywords electrochemical characterization, impedance spectroscopy, laser doppler anemometry (LDA), solid oxide fuel cells (SOFC), vacuum plasma spraying (VPS)

1. Introduction

Solid oxide fuel cells (SOFCs) electrochemically convert the chemical energy of fuel gases (H₂, CO, CH₄, and other hydrocarbons) in the reaction with oxygen into electrical power. In comparison to power generation by means of combustion processes, the electrochemical oxidation of the fuel gases in a SOFC leads to higher overall efficiencies with very low harmful emissions.^[1-3]

The cell consists of a porous (La, Sr) MnO₃-cathode, a gas tight oxygen ion conductive yttria- or scandia-stabilized ZrO₂ (YSZ, ScSZ) electrolyte, and a porous ZrO₂/Ni-anode. In the first generation of planar SOFCs, an approximately 150 μm thick solid electrolyte has been necessary in order to support the cell mechanically. Because of this high thickness and the strong dependence of the ionic conductivity of the ZrO₂ with temperature, the cells are usually operated between 900 to 1000 °C. The high thermal load of the materials can result in detrimental diffusion and evaporation processes with a strong reduction of the cell performance and reduced long-term stability. Another disadvantage of the electrolyte supported cells is the low fracture toughness of the zirconia, the danger of crack formation, and, hence, the very limited size of the cells that can be fabricated reliably.

M. Lang, R. Henne, S. Schaper, and G. Schiller, Institut für Technische Thermodynamik, Deutsches Zentrum für Luft- und Raumfahrt, D-70569 Stuttgart, Germany. Contact e-mail: michael.lang@dlr.de.

In order to increase stability, life time, and economy, the operating temperature of the cells has to be reduced to about 700 to 800 °C. For this purpose, it is necessary to decrease the overall thickness of the SOFC and particularly of the electrolyte. This means that a relatively thick electrolyte no longer serves as the “backbone” of a cell. With this second generation SOFC characterized by a thin-film electrolyte, an additional component is required that has the function to mechanically stabilize the cell. A novel concept for a metallic substrate supported thin-film SOFC (Fig. 1) has been developed at DLR Stuttgart. In the DLR concept, the entire cells will be fabricated by an integrated multistep plasma deposition procedure, mainly based on specifically adapted vacuum plasma spraying (VPS) processes. This fabrication technique enables the deposition of thin, dense electrolyte layers as well as of controlled porous electrodes in a consecutive spray process. High material deposition rates promise inexpensive and fast cell production, especially in the case when large active cell areas are required. Low internal resistances in the plasma-sprayed cells lead to high power densities and enable the reduction of operating temperature without a significant decrease in performance. Consequently, the long-term stability can be improved and less expensive materials can be used.

2. Experimental

2.1 Fabrication of the Cells

The VPS technique and the equipment used at the DLR Stuttgart have been described in detail elsewhere.^[4] Therefore, only some characteristic features of the DLR installation, which

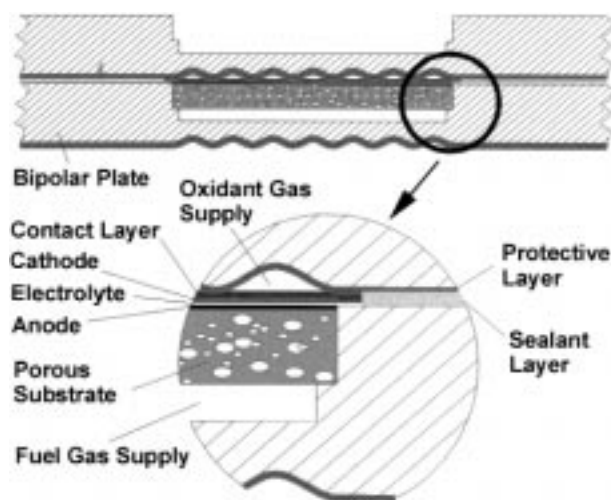


Fig. 1 Principle of the SOFC design according to the DLR spray concept

are essential for the manufacture of SOFC components, are emphasized. Novel plasma torches with Laval-like nozzle contours for supersonic plasma jet velocities of up to 2000 to 3000 m/s have been developed,^[5,6] resulting in enhanced spray particle velocities of up to 800 to 900 m/s (*e.g.*, Al_2O_3) and improved spray conditions to achieve thin but still very dense electrolyte layers.^[7] The internal powder injection by several integrated powder injection ports at different positions along the nozzle allows the spraying of very different materials simultaneously, thus enabling the production of structured composite coatings such as graded cermet layers.

Controlled porous electrode layers can be obtained by appropriate selection of the composition, the morphology, and the grain size fraction of the spray powders (Table 1 and Fig. 2) and by carefully adjusting the spray parameters (Table 2). The optimization of the VPS parameters has been supported by laser doppler anemometry (LDA) investigations, which allow the evaluation of velocities and trajectories of spray particles.^[8] A robot-controlled movement of the spray torch ensures uniform and reproducible deposition of the layers. An electrical heating device, which has been developed for operation in vacuum conditions, is applied to heat the substrates prior to coating in order to diminish the thermal gradients during deposition. The temperature of substrates was controlled with thermocouples.

Table 1 lists the SOFC powders used for the fabrication of the cells. Figure 2 shows their corresponding morphologies.

The first step of the development of the sprayed cells focused on optimization of the single electrode and electrolyte layers in terms of microstructure, electrical conductivity, and electrochemical activity. The anodes were sprayed by combining the NiO with the YSZ or the ScSZ powder. In the case of the cathodes, $(\text{La}_{0.8}\text{Sr}_{0.2})_{0.98}\text{MnO}_3$ powder (LSM) was sprayed together with YSZ or ScSZ, respectively, for the electrocatalytic layers. An additional layer of pure LSM acts as a current collector. The high melting YSZ and ScSZ ceramic powders were injected internally, while the lower melting NiO and LSM powders were fed externally of the nozzle into the

plasma. The desired layer composition was obtained by adjusting the powder feed rates.

In order to develop the spray parameters (Table 2) and to evaluate the resulting qualities of the layers separately, the electrode and electrolyte layers were sprayed onto different substrates. For the determination of the electrical conductivity, nonconductive alumina substrates were used, and for the evaluation of the electrochemical activity of the electrodes, the anodes and cathodes were sprayed onto sintered YSZ electrolytes (Kerfol, Eschenbach Opf., Germany).^[9] The sintered electrolytes had been screen printed with the corresponding counter electrode at Siemens AG (Erlangen, Germany) prior to the spray process. This enables us to individually characterize the VPS-fabricated electrodes separately from the other cell components and to run the cells at technical current densities of about 200 to 1000 mA/cm^2 .

The completely sprayed cells were deposited onto different metallic substrates, *e.g.*, porous plates made of chromium-based alloy Cr-5 wt.% Fe-1 wt.% Y_2O_3 (Plansee, Reutte, Austria) or of stainless steel (GKN Sinter Metal Filters, Radevormwald, Germany) and nickel felts (Medicoat, Switzerland). The spray parameters for the fabrication of the cells are listed in Table 2. More details on the plasma spray process applied for the production of SOFC components are given in Ref 10 and 11.

2.2 Characterization of the Cells

Figure 3 presents an overview of the different characterization methods of the cells and cell components, which can be divided into microstructural, electrical, and electrochemical investigations. This indicates the overall quality of the single cell components and enables iterative improvement of the cells by parameter variation of the VPS processes.

The test equipment for the electrochemical characterization of the cells at DLR Stuttgart consists of furnaces, operation control units, data acquisition systems, and a frequency response analyzer.

3. Results and Discussion

3.1 Anode Development

The optimization procedure of the spray parameters has been supported by LDA measurements. Figure 4 shows an example of the trajectories of the anode powders in the plasma jet for the fabrication of porous electrode layers.

A careful adjustment of the carrier gas flow rate is necessary to inject a high amount of the powder into the hot core of the plasma jet to realize a sufficient powder melting and a high deposition rate. It has been shown that the particle velocities depend strongly on spray parameters such as type of torch nozzle, gas composition, chamber pressure, and torch power. With the spray parameters listed in Table 2, particle velocities between 380 m/s at a distance of 50 mm and 250 m/s at a distance of 240 mm were measured for spraying of the anode layer. The relatively low velocity of the particles at impact on the substrate leads to the desired formation of porous electrodes.

The NiO in the anode is reduced by hydrogen to pure Ni at operating conditions of the cells. This leads to a further increase in porosity to about 21 vol.%, which ensures sufficiently high

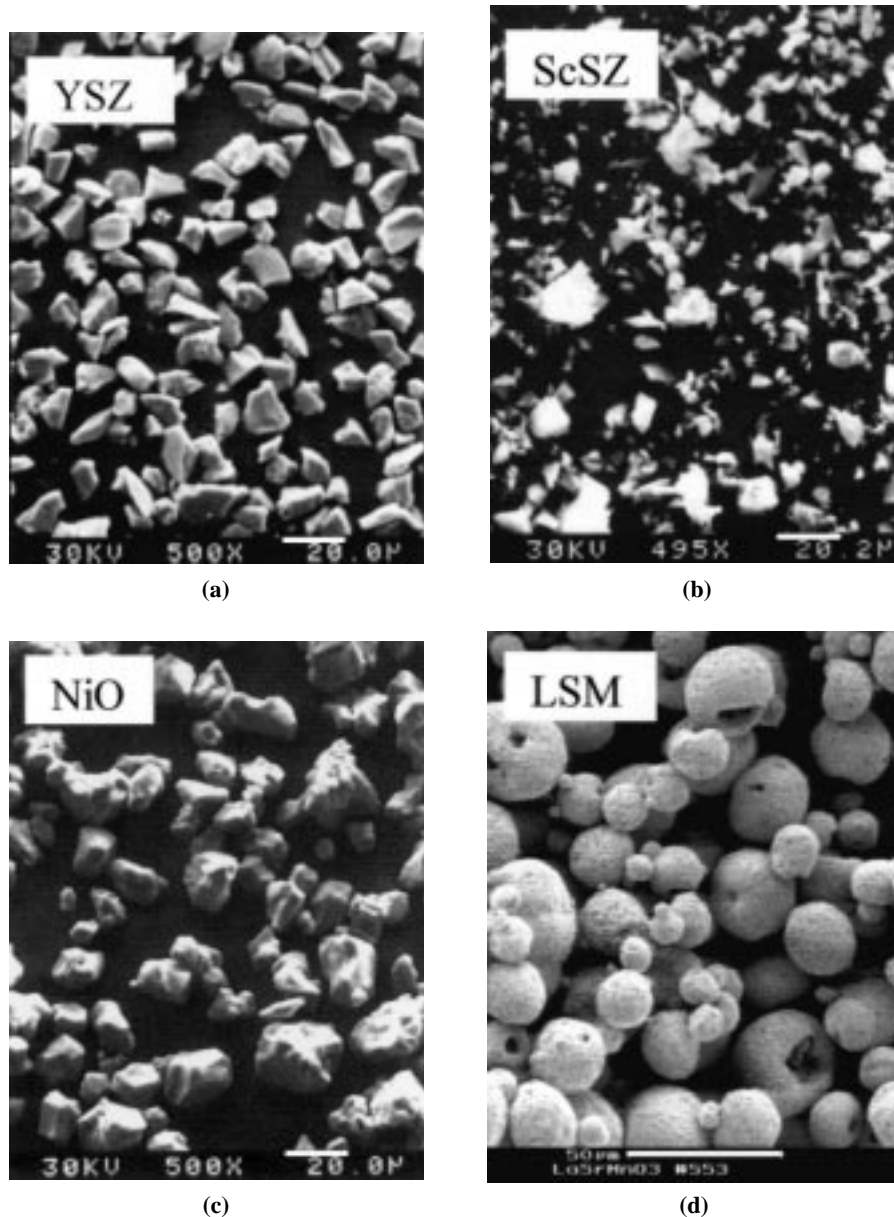


Fig. 2 Powders used for the fabrication of the SOFCs (above: YSZ and ScSZ electrolyte powder; below: NiO anode and LSM cathode powder)

Table 1 Description of the powders used for the spraying of the SOFC layers

Powder	NiO	ZrO ₂ -7 mol.% Y ₂ O ₃	ZrO ₂ -10 mol.%Sc ₂ O ₃	(La _{0.8} Sr _{0.2}) _{0.98} MnO ₃
Short name	NiO	YSZ	ScSZ	LSM
Morphology	Sintered, crushed	Sintered, crushed	Sintered, crushed	Sintered, spherical
Size distribution	10–25 μm	5–25 μm	2–35 μm	20–40 μm
Supplier	Cerac (Milwaukee, WI)	Medicoat (Niederrohrdorf, Switzerland)	Siemens (Erlangen, Germany)	EMPA (Dübendorf, Switzerland)

gas diffusion. Figure 5 shows the corresponding pore size distribution, measured with mercury intrusion porosimetry. In contrast to other porosimetry determination systems (*e.g.*, quantitative image analysis), mercury intrusion porosimetry is suitable to also detect pores less than 1 μm.

The pore size distribution of the plasma-sprayed and reduced YSZ + NiO-anode ranges from 0.03 to 20 μm, with a maximum at about 0.5 μm. The smaller pores are formed by the reduction of NiO, whereas the larger pores are created during the spray process.

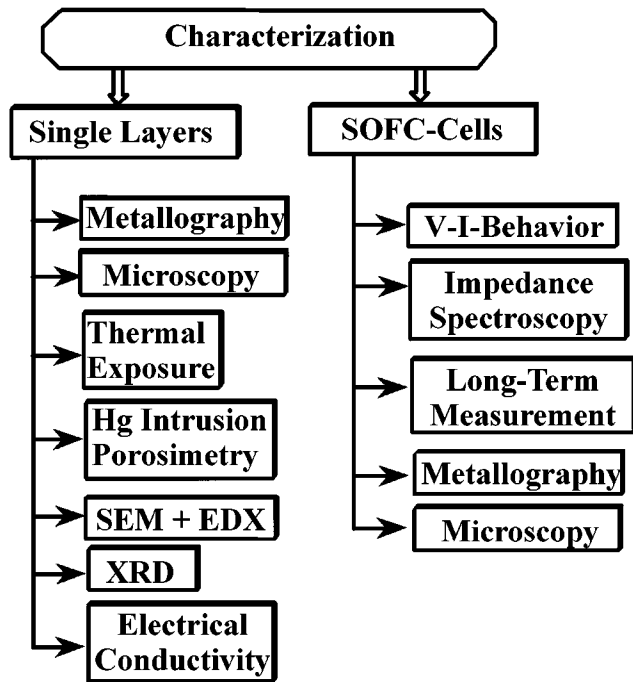
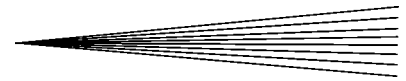


Fig. 3 Characterization methods for the cells

Table 2 VPS parameters for the fabrication of the cells

Spray parameters	Anode	Electrolyte	Cathode
Powders	YSZ + NiO ScSZ + NiO	YSZ ScSZ	YSZ + LSM ScSZ + LSM
Torch nozzle	Mach 3 Laval(a) (7 mm)	Mach 3 Laval(a) (7 mm)	F4V-standard (7 mm)
Torch power	30 kW	30 kW	30 kW
Plasma gas composition	Ar/H ₂ /He	Ar/H ₂	Ar/He
Chamber pressure	200 mbar	100 mbar	200 mbar
Spray distance	240 mm	230 mm	180 mm
Thickness	30–40 μm	20–30 μm	20–30 μm

(a) Developed at DLR

3.2 Electrolyte Development

For the production of high performance SOFCs, it is necessary to spray thin gas tight electrolyte layers with high material deposition efficiencies. These requirements are best achieved by completely melting the powder particles. These are then accelerated to a high speed in the plasma jet and, therefore, flattened to form dense lamellae on impact upon the substrate. Figure 6 shows the measured particle velocities (LDA) of the YSZ electrolyte powder (Fig. 2), which was sprayed with a conventional conical F4V nozzle, and a Mach 3 Laval nozzle, developed at DLR.

The velocities of the particles sprayed with the Mach 3 Laval nozzle increase to about 650 m/s, whereas the particle velocities of the standard nozzle are in the range of 450 m/s. With the utilization of the Laval nozzles of DLR,^[4,5] the temperature and velocity profiles of the laminar hot plasma jet are broadened and elongated. This leads to an increase of the heat and momentum transfer to the ceramic particles, thereby resulting in completely

molten particles with high velocities. Therefore, the formation of a dense lamellar microstructured electrolyte layer with high interparticle bonding can be achieved.

Figure 7 shows the measured deposition rates and porosities of two YSZ electrolyte layers, which were produced with the Mach 3 Laval nozzles using different plasma gas compositions (see also Table 2) as a function of the distance from the nozzle. Both deposition rates decrease from about 8 μm/pass at a distance from the nozzle of 220 mm to 6 μm/pass at a distance of 250 mm (Fig. 7). Similar results were achieved with the ScSZ electrolyte.

The porosities, measured by quantitative image analysis, of the electrolyte layers are in the range of 1.5 to 2.5 area% and indicate the closed porosity. The lowest porosity of about 1.6 area% was obtained with the 40Ar/6H₂ plasma gas composition at a spray distance of 230 mm. Due to the high content of H₂, the plasma enthalpy and thermal conductivity are increased and a higher fraction of the YSZ particles is sufficiently melted and deposited on the substrate. With a plasma gas composition of 38Ar/2H₂/20He (SLPM), the porosity values, especially at larger spray distances, are slightly higher.

3.3 Cathode Development

The plasma-sprayed YSZ + LSM cathodes were optimized in a similar way as the anodes. The variation of the spray parameters has shown that the perovskite of the cathode tends to decompose, especially in the case when H₂ is added to the plasma gas. With the spray parameters listed in Table 2, cathodes can be sprayed without decomposition (Fig. 8) at deposition rates as high as 4 to 5 μm/pass.

The lack of a “pore forming process” leads to a lower overall porosity in the LSM + YSZ cathodes in comparison to the anodes. Actual development focuses on the usage of alternative cathode powders, the application of pore formers, and a further optimization of the spray parameters.

3.4 Cell Development

Figure 9 shows the cross section of a completely plasma-sprayed SOFC consisting of a NiO + YSZ anode, a YSZ electrolyte, and a double-layered LSM + YSZ/LSM cathode. These layers were consecutively sprayed onto a porous metallic substrate.

The plasma-sprayed YSZ electrolyte exhibits a dense lamellar microstructure, whereas the anode has a fine open porosity of 21 vol.% after the reduction of the NiO. The overall porosity of the cathode reaches only about 10 vol.% with relatively coarse pores. Recent developments aim at improving the cathode’s microstructure and at optimization of the thicknesses of the layers.

3.5 Scale-up of the Cells

The first plasma-sprayed cells for the electrochemical characterization were of a diameter 35 mm and had active cell areas of 5 cm². In the next steps of development, the diameter of the cells was increased to 48 and 96 mm. These cells were also used for single cell measurements. Preheating of the substrates prior to the deposition process diminishes thermal stresses in the plasma-sprayed layers. For the assembling of SOFC stacks,

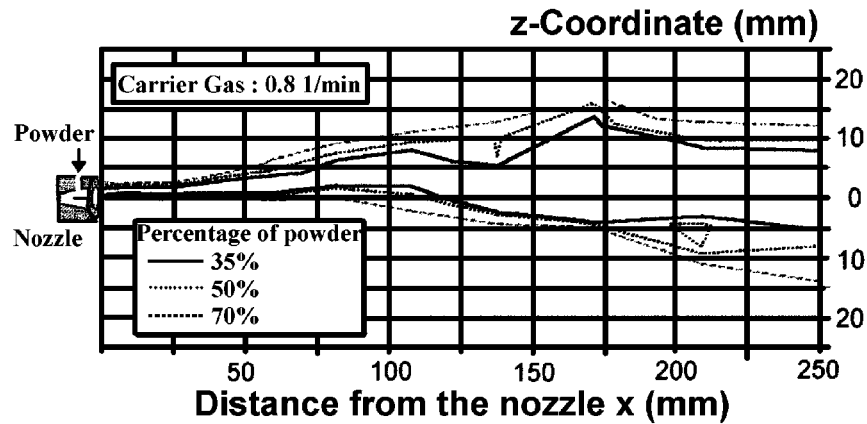


Fig. 4 Trajectories of the SOFC YSZ powder in the plasma jet (for spray parameters, see Table 2)

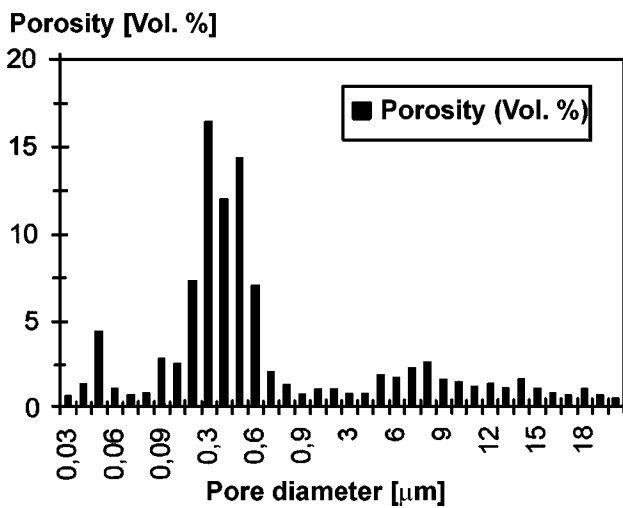


Fig. 5 Pore size distribution of a plasma-sprayed and reduced NiO + YSZ SOFC anode

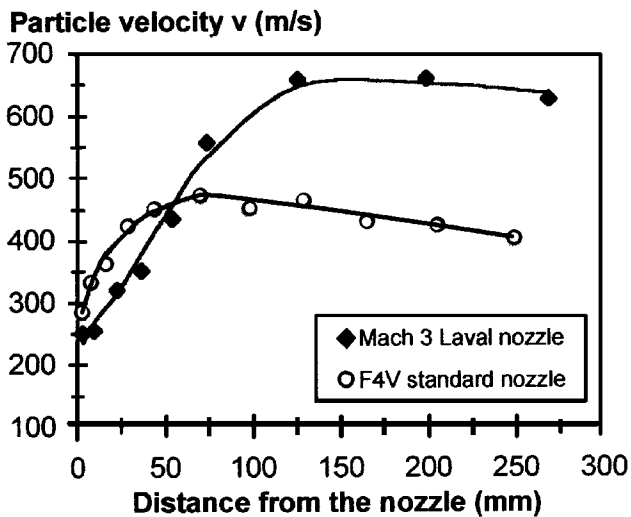


Fig. 6 Velocities of the YSZ powder, sprayed with different plasma nozzles

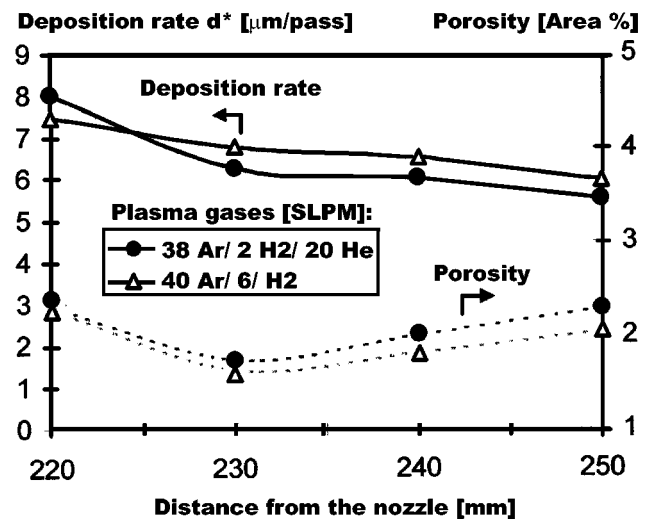


Fig. 7 Deposition rate and porosity of plasma-sprayed YSZ electrolytes

square cells with 100×100 mm and 200×200 mm with active areas up to 300 cm^2 were produced.

3.6 Electrical Characterization

The overall ohmic resistances of the cells are a sum of the contact resistances and the ohmic resistances of the cell layers. Figure 10 shows the electrical conductivity of the plasma-sprayed layers as a function of temperature.

The electronic conductivities of the electrodes are 3 to 4 orders of magnitude higher than the oxygen ion conductivities of the electrolytes. Because of the high mobility of the electrons in the Ni phase, the reduced NiO + YSZ anode shows a high electronic conductivity. Due to the lamellar microstructure, the conductivity of the sprayed anode is higher compared to sintered anodes of the same material composition.^[12] As expected for metals, the electronic conductivity decreases with temperature. It can be suggested that the fine porous and highly electronically conducting anode structure exhibits extended three-phase boundaries (Ni/YSZ/pore) where the electrochemical reaction takes place.

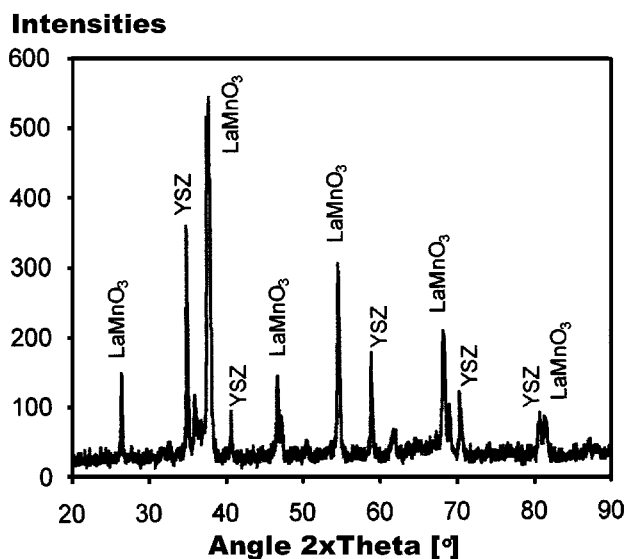


Fig. 8 X-ray diffraction pattern of a plasma-sprayed LSM + YSZ cathode (for parameters, see Table 2)

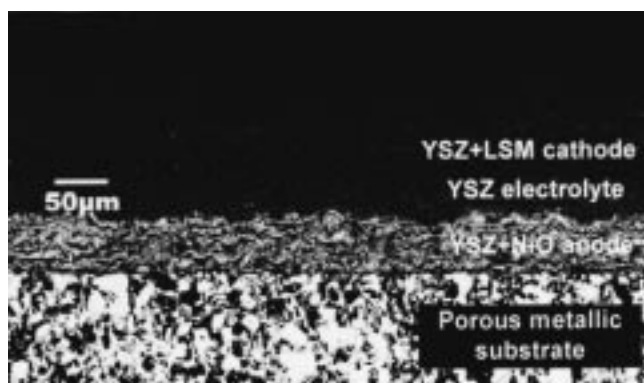


Fig. 9 Cross section of a plasma-sprayed SOFC (for spray parameters, see Table 2)

The conductivity of the plasma-sprayed LSM cathode is higher than that of the corresponding LSM + YSZ cathode, in which the YSZ contributes very little to the overall conductivity. Due to an intrinsic *p*-type conduction mechanism, the conductivities of both cathodes gradually increase with temperature. The ionic conductivity of the ScSZ electrolyte is about twice as high as that of the YSZ electrolyte. The increase of ionic conductivity with temperature is due to the enhanced diffusion of O^{2-} vacancies in the cubically stabilized structures.

3.7 Electrochemical Characterization

The electrochemical performance of the first plasma-sprayed cells was poor because the porosities in the electrodes were too low and the thicknesses of the cell layers were not adapted. Reduction of the electrolyte thickness to about 40 μm leads to an increase in the electrical power density of the cells. The use of improved cathode and anode powders enabled the optimization of the electrodes' microstructure and further increased the power

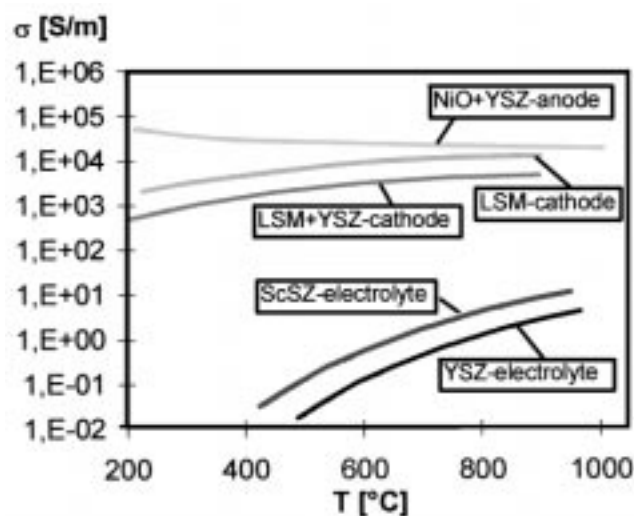


Fig. 10 Electrical conductivity of the plasma-sprayed cell layers

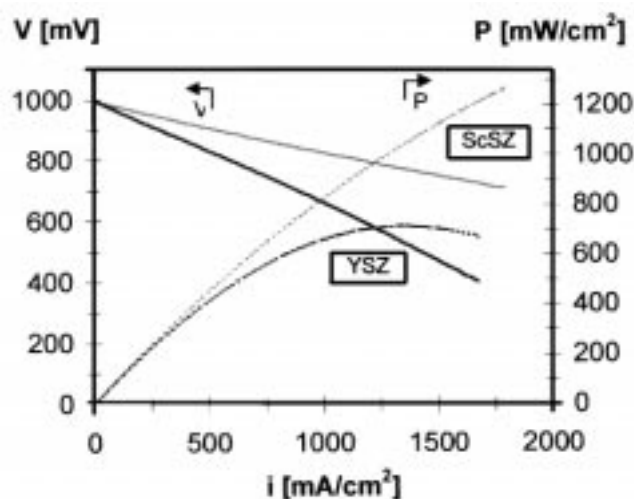


Fig. 11 I-V behavior of a plasma-sprayed SOFC using YSZ and ScSZ as electrolyte material (operating gases: 0.5 SLPM H_2 , 0.5 SLPM O_2 , and temperature: 900 °C)

density. In the case of the electrolyte, the YSZ was replaced by ScSZ.

A comparison of two cells fabricated with YSZ and ScSZ as electrolyte powder is depicted in Fig. 11. The cells with active areas of 5 cm^2 were sprayed onto porous nickel felts and operated at 900 °C with hydrogen and oxygen as process gases.

The use of ScSZ as the electrolyte powder, with a higher ionic conductivity compared to YSZ, leads to a high power density cell of about 1260 mW/cm^2 (700 mV, 1800 mA/cm^2). A similar cell fabricated with YSZ resulted in a power density of approximately 630 mW/cm^2 (700 mV, 900 mA/cm^2).

For the basic experiments and developments, O_2 and H_2 were used to evaluate the cell characteristics; whereas for technical application, the SOFCs will be operated with air and hydrogen. Figure 12 shows the corresponding I-V curves of a plasma-sprayed cell that was fabricated with NiO, ScSZ, and LSM (5 cm^2). The flow rates of the operating gases used were 0.5 SLPM H_2 and 1.5 SLPM air.

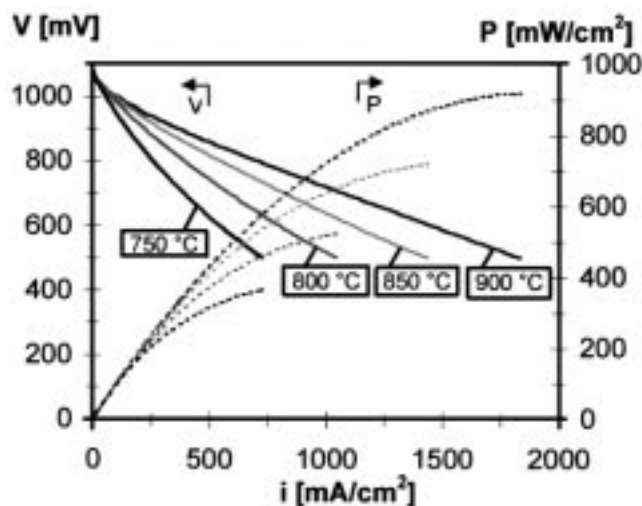


Fig. 12 I-V behavior of a plasma-sprayed SOFC at different temperatures (operating gases: 0.5 SLPM H₂ and 1.5 SLPM air)

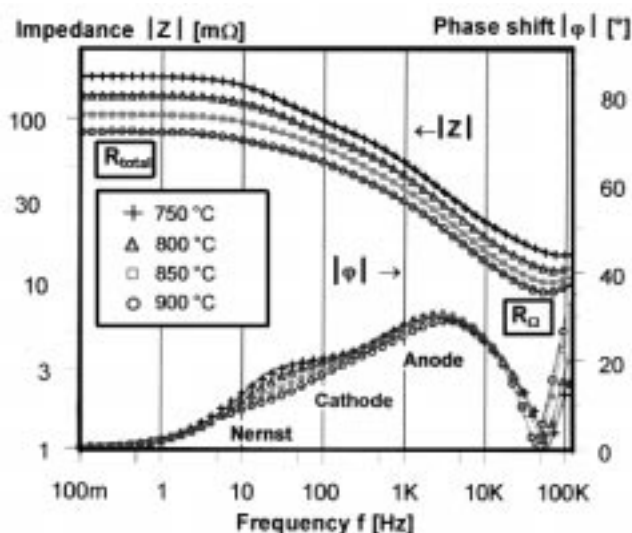


Fig. 13 Impedance spectra of a plasma-sprayed SOFC (H₂, air, and 750 to 900 °C)

When using air instead of oxygen, the lower oxygen partial pressure at the cathode reduces the performance of the cells by about 35%. Nevertheless, this cell still reached high power densities, P , at a cell voltage of 0.7 V of 750 mW/cm² at 900 °C (1075 mA/cm²), 570 mW/cm² at 850 °C (825 mA/cm²), 410 mW/cm² at 800 °C (600 mA/cm²), and 280 mW/cm² at 750 °C (400 mA/cm²). The maximum power densities—at lower cell voltages—were approximately 150 mW/cm² higher.

In order to evaluate the voltage losses of the different cell components, impedance spectroscopy was performed. With this technique, a potentiostat with an alternating voltage of 5 to 10 mV and variable frequencies between 10 mHz and 4 MHz was applied to the cell. A frequency response analyzer monitors the corresponding current signal of the cell. From the phase shift between voltage and current, the complex resistance (impedance) can be calculated. Figure 13 shows the impedance spectra of a cell, consisting of a NiO + ScSZ

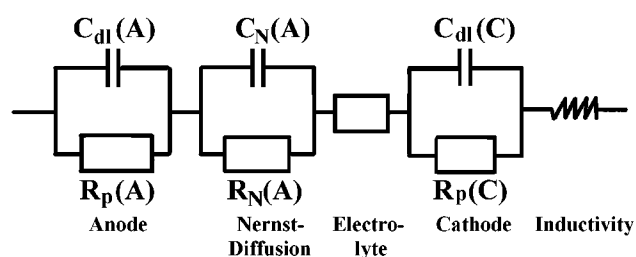


Fig. 14 Equivalent circuit of a SOFC

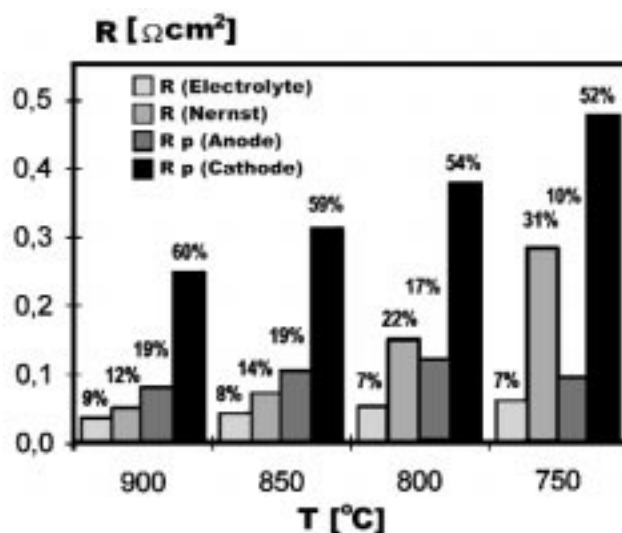


Fig. 15 Impedance values of a plasma-sprayed SOFC (0.5 SLPM H₂, 1.5 SLPM air, and 750 to 900 °C)

anode, a ScSZ electrolyte, and a LSM + ScSZ cathode, measured at a current density of 200 mA/cm² at different temperatures. The impedance values in the high frequency range correspond to the ohmic resistance, and the impedance values in the low frequency range correspond to the overall resistance of the cell.

The measured spectra show very low ohmic impedances, R_{Ω} , in the high frequency range and low total impedances, R_{total} , in the low frequency range. The ohmic resistances change from 8 mΩ at 900 °C to only 12 mΩ at 750 °C, while the total area specific resistances range from 85 mΩ (900 °C) to 180 mΩ (750 °C).

Three frequency-dependent processes can be detected in the impedance spectra: The polarization resistances at the anode, $R_p(A)$, and the cathode, $R_p(C)$, appear in the high and the middle frequency ranges, respectively. In the low frequency range, a third impedance is registered, which is attributed to the diffusion of H₂ and produced H₂O at the anode side. Figure 14 shows the corresponding equivalent circuit to describe the electrochemical behavior of the cells. The diffusion process is taken into account by the Nernst term, $R_N - C_N$. The individual resistances calculated by fitting of the equivalent circuit to the measured impedance spectra at the different temperatures (750 to 900 °C) are depicted in Fig. 15. The current density is 200 mA/cm².

The thin plasma-sprayed ScSZ electrolyte contributes very little to the overall resistance. The relative losses decrease from 9% at 900 °C to only 7% at 750 °C. The polarization resistance

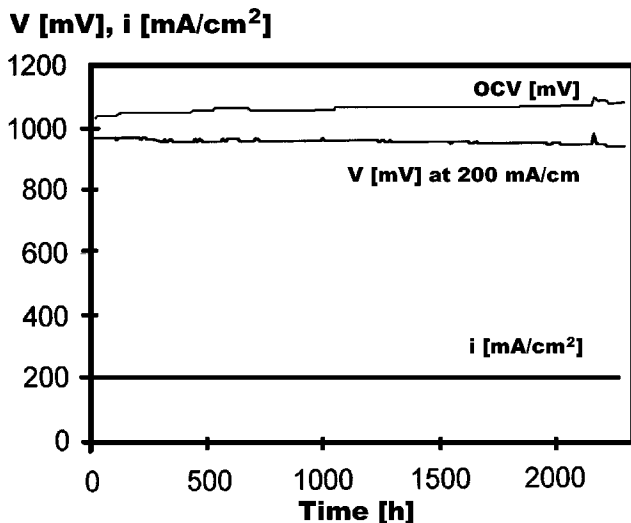
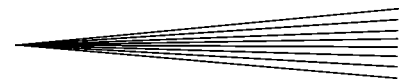


Fig 16 Long-term measurement of a plasma-sprayed SOFC (0.5 SLPM H_2 , 0.5 SLPM O_2 , 900 °C, and 200 mA/cm²)

of the porous anode, $R_p(\text{Anode})$, remains at around 0.1 Ωcm^2 for the entire temperature range, which is also very low.

The diffusion resistance, $R(\text{Nernst})$, increases in the measured range from 0.05 to 0.28 Ωcm^2 with decreasing temperature. The highest losses are caused through the polarization resistance of the cathode, which is in the range of 0.25 to 0.47 Ωcm^2 (50 to 60%). Further improvement of the microstructure, especially an increase in the porosity by further developed spray parameters and powders (pore formers), is expected to lower the polarization resistance of the plasma-sprayed cathodes.

A second approach to improve cathode porosity pursued at DLR Stuttgart is the development of porous cathodes by *in-situ* synthesis of $(\text{La}, \text{Sr})\text{MnO}_3$ produced by injection of cheap liquid precursors consisting of solved salts or suspensions into the hot core of a plasma generated in a high frequency torch. In the first spray experiments, almost pure LaMnO_3 layers with columnar crystal growth and high porosity were fabricated.^[13]

3.8 Long-Term Stability

Figure 16 shows the long-term measurement at 200 mA/cm² and 900 °C with H_2 and O_2 as operating gases. During the 2000 operation hours of the SOFC, the degradation of the cell voltage was in the range of 1% per 1000 h. Further improvement concerning stability can be achieved by lowering the operating temperature and modifying the microstructure of the electrodes.

4. Conclusions

The VPS technique has proved to be a very useful material processing tool for producing the entire SOFC assembly. In contrast to sintering techniques, thin-film SOFCs with material and porosity gradients can be produced with the plasma spraying technique in only one consecutive process. The plasma spray technology has high potential to be developed into a continuous mass production process for the cells. In such a production line, the different cell layers are deposited in different chambers,

which are connected to each other with vacuum locks. Cost estimations for the continuous fabrication of the cells in such a multichamber installation with several plasma torches revealed a significant cost reduction.

The cells show very good electrochemical performance and low internal resistances. Power densities of 300 to 400 mW/cm² at reduced operating temperatures of 750 to 800 °C were achieved. These values are comparable to the best values achieved with sintered cells.^[14]

The use of the plasma-sprayed cells allows the reduction of the operating temperature of the SOFC to below 800 °C with higher long-term stability and lowered production costs. Further developmental work will concentrate on improving the layers' microstructures and thus the electrochemical performance of cells up to a size of 200 × 200 mm. Stacks with several cells of this size will be assembled and investigated in short-term and long-term operation in order to obtain information about stack performance and durability.

References

1. S.E. Veyo and C.A. Forbes: *3rd Eur. Solid Oxide Fuel Cell Forum 1998*, Nantes, France, P. Stevens, ed., U. Bossel, Oberrohrdorf, Switzerland, 1998, vol. 1, pp. 79-86.
2. M. Peht: *Int. Conf. with Exhibition Fuel Cell 2000*, Lucerne, Switzerland, L. Blomen, ed., U. Bossel, Oberrohrdorf, Switzerland, pp. 367-78.
3. N.Q. Minh and T. Takahashi: in *Science and Technology of Ceramic Fuel Cells*, Elsevier-Verlag, Amsterdam, 1995, pp. 331-49.
4. G. Schiller, R. Henne, and V. Borck: *J. Thermal Spray Technol.*, 1995, vol. 4 (2), pp. 185-94.
5. R. Henne, W. Mayr, and A. Reusch: *Thermische Spritzkonferenz 1993*, Aachen, Germany, *DVS-Berichte*, D. von Hofe and E. Lugscheider, eds., DVS-Verlag GmbH, Düsseldorf, 1993, vol. 152, pp. 7-11 (in German).
6. R. Henne, V. Borck, D. Siebold, W. Mayr, A. Reusch, M. Rahmane, G. Soucy, and M. Boulos: *3rd Eur. Congr. on Thermal Plasma Processes 1994*, Aachen, Germany, *VDI-Berichte*, D. Neuschütz, ed., VDI-Verlag GmbH, Düsseldorf, 1995, vol. 1166, pp. 247-66.
7. S. Schaper: "Entwicklung und Elektrochemische Charakterisierung von Vakuumplasmagespritzten $ZrO_2\text{-}Y_2O_3$ -Festelektrolyten für die Hochtemperaturbrennstoffzelle (SOFC)," Diploma Thesis, University of Siegen, performed at DLR Stuttgart, Stuttgart, 1998 (in German).
8. W. Mayr, K. Landes, and A. Reusch: *Thermische Spritzkonferenz 1993*, Aachen, Germany, *DVS-Berichte*, D. von Hofe and E. Lugscheider, eds., DVS-Verlag GmbH, Düsseldorf, 1993, vol. 152, pp. 143-47 (in German).
9. M. Lang: *Fortschritt-Berichte VDI, Reihe 6: Energietechnik*, VDI-Verlag GmbH, Düsseldorf, 2000, No. 435 (in German).
10. R. Henne, M. Lang, M. Müller, R. Ruckdäschel, G. Schiller: *2nd Int. Symp. on Heat and Mass Transfer under Plasma Conditions 1999*, Antalya, Turkey, P. Fauchais, J. van der Mullen, and J. Heberlein, eds., The New York Academy of Science, New York, NY, 1999, pp. 124-36.
11. G. Schiller, R. Henne, and M. Lang: *3rd Eur. Solid Oxide Fuel Cell Forum 1998*, Nantes, France, P. Stevens, ed., U. Bossel, Oberrohrdorf, Switzerland, 1998, vol. 1, pp. 123-32.
12. D.W. Dees, T.D. Claar, T.E. Esler, D.C. Fee, F.C. Mrazek: *J. Electrochem. Soc.*, 1987, vol. 134 (9), pp. 2141-46.
13. G. Schiller, E. Bouyer, M. von Bradke, R. Henne, M. Müller: *Surface Engineering*, Proc. Euromat 1999, H. Dimigen, ed., Wiley-VCH Verlag, Weinheim & DGM, 2000, vol. 11, pp. 300-05.
14. H.J. Beie, L. Blum, W. Drenckhahn, H. Greiner, H. Schichl: *3rd Eur. Solid Oxide Fuel Cell Forum 1998*, Nantes, France, P. Stevens, ed., U. Bossel, Oberrohrdorf, Switzerland, 1998, vol. 1, pp. 3-14.